Nuclear Science and Techniques (2023) 34:34
https://doi.org/10.1007/s41365-023-01191-6

Conceptual design and safety characteristics of a new multi-mission high flux research reactor

Wei Xu[1] · Jian Li[2] · Heng Xie[2] · Zhi-Hong Liu[2] · Jing Zhao[2] · Fei Xie[2] · Lei Shi[2]

Received: 8 November 2022 / Revised: 19 December 2022 / Accepted: 3 January 2023 / Published online: 16 March 2023

Abstract

Research reactors with neutron fluxes higher than 10^{14} n cm^{-2} s^{-1} are widely used in nuclear fuel and material irradiation, neutron-based scientific research, and medical and industrial isotope production. Such high flux research reactors are not only important scientific research facilities for the development of nuclear energy but also represent the national comprehensive technical capability. China has several high flux research reactors that do not satisfy the requirements of nuclear energy development. A high flux research reactor has the following features: a compact core arrangement, high power density, plate-type fuel elements, a short refueling cycle, and high coolant velocity in the core. These characteristics make it difficult to simultaneously realize high neutron flux and optimal safety margin. A new multi-mission high flux research reactor was designed by the Institute of Nuclear and New Energy Technology at Tsinghua University in China; the reactor can simultaneously realize an average neutron flux higher than 2.0×10^{15} n cm^{-2} s^{-1} and fulfill the current safety criterion. This high flux research reactor features advanced design concepts and has sufficient safety margins according to the preliminary safety analysis. Based on the analysis of the station blackout accident, loss of coolant accident, and reactivity accident of a single-control drum rotating out accidently, the maximum temperature of the cladding surface, minimum departure from nucleate boiling ratio, and temperature difference to the onset of nucleate boiling temperature satisfy the design limits.

Keywords High flux research reactor · Neutron flux · Safety analysis · Maximum temperature of cladding surface · Departure from nucleate boiling ratio

List of symbols

A	Flow area, m^2
A_H	Heated area, m^2
G	Mass flux, kg m^{-2} s^{-1}
G^*	Dimensionless mass flux, $G^* = \frac{G}{\sqrt{\lambda(\rho_l-\rho_g)\rho_g g}}$
g	Acceleration of gravity, m s^{-2}
ρ_l, ρ_g	Density of liquid and gas, kg m^{-3}
$\overline{\rho}$	Average density of hot coolant and cold coolant, kg m^{-3}
W	Channel width of rectangular channel, m
λ	Critical wavelength $\lambda = \sqrt{\frac{\sigma}{(\rho_l-\rho_g)g}}$
σ	Surface tension, N m^{-1}
ΔT_{sub}	Subcooling, K
ΔT^*_{sub}	Dimensionless subcooling, $\Delta T^*_{sub} = \frac{C_p \Delta T_{sub}}{h_{fg}}$
q_{CHF}	Critical heat flux (CHF), Kw m^{-2}
q^*_{CHF}	Dimensionless CHF, $q^*_{CHF} = \frac{q_{CHF}}{h_{fg}\sqrt{\lambda(\rho_l-\rho_g)\rho_g g}}$
T_w	Wall temperature, K
T_s	Saturation temperature, K
P	Pressure, MPa
Re	Reynolds number
Pr	Prandtl number
$\dot{m}$	Mass flow rate of natural circulation, kg s^{-1}
ΔP_d	The driving head, Pa
ΔP_{el}	Elevation pressure drop, Pa
F	Drag loss coefficient along the path
ξ	Local drag loss coefficient

✉ Lei Shi
shlinet@tsinghua.edu.cn

[1] School of Nuclear Science and Engineering, Beijing Key Laboratory of Passive Safety Technology for Nuclear Energy, North China Electric Power University, Beijing 102206, China

[2] Institute of Nuclear and New Energy Technology, Collaborative Innovation Center of Advanced Nuclear Energy Technology, Key Laboratory of Advanced Reactor Engineering and Safety of Ministry of Education, Tsinghua University, Beijing 100084, China

ξ_{tol}	Total drag loss coefficient
De	Equivalent diameter, m
Q_{nc}	Decay heat, MW
R_f	The fuel fission reaction rate, n cm^{-3} s^{-1}
Σ_f	Macroscopic fission cross section, cm^{-1}
σ_f	Microscopic fission cross section, cm^2
N	The number density, cm^{-3}
ϕ	The neutron flux, n cm^{-2} s^{-1}
P_d	The average power density, W cm^{-3}
Q_y	The irradiation ability per year, cm a^{-1}
Q_d	The irradiation ability per day, cm a^{-1}
V	The volume of irradiation space, cm^3
t	The irradiation time, d

1 Introduction

Commercial water reactors can usually reach a neutron flux level of 10^{14} n cm^{-2} s^{-1}. Neutron-based scientific research, isotope production, and material and fuel irradiation typically require a neutron flux of at least 10^{14} n cm^{-2} s^{-1}. Therefore, high flux research reactors that can supply fast or thermal neutron fluxes of at least 10^{14} n cm^{-2} s^{-1} are in high demand worldwide. The high flux research reactor is not only an important experimental research facility for the development of nuclear energy but also a representative of the national comprehensive technical capability. High flux research reactors can supply, for example, sufficient neutron flux for fuel and material testing and efficient production of industrial and medical isotopes. Although some other researched reactors [1, 2] have also been studied to yield radioisotopes or for other uses, high flux research reactors continue to play an important role in the development of nuclear energy.

The USA has two important high flux research reactors: a high flux isotope reactor (HFIR) and an advanced test reactor (ATR). The HFIR is in the Oak Ridge National Laboratory, with a maximum design thermal power of 100 MW [3], which reached the first criticality on August 25, 1965. The maximum neutron flux in the center channel of the HFIR is higher than 10^{15} n cm^{-2} s^{-1} [3]. The original goal of HFIR was heavy isotope production. However, owing to the spatially varying neutron energy distribution, its application has expanded to neutron-focused scientific research, such as studies on matter structure, neutron damage to materials, and neutron activation analysis. One large flux trap is in the center core that can be configured to suit various tests and several reflector irradiation channels for additional material or fuel element irradiation [4].

The ATR is in Idaho National Laboratory (INL), and the designed thermal reactor power is 250 MW. The peak thermal neutron flux can reach 1.0×10^{15} n cm^{-2} s^{-1} in the core [5, 6]. The ATR is currently operated at approximately 110 MW and can provide a thermal neutron flux of 4.4×10^{14} n cm^{-2} s^{-1} and maximum fast ($E>1.0$ MeV) neutron fluxes of 2.2×10^{14} n cm^{-2} s^{-1} [7]. The ATR is the only research reactor in the USA that can provide large-volume, high-flux neutron irradiation in a prototype environment. The ATR makes studying the effects of intense neutron and gamma radiation on reactor materials and fuels possible. The ATR can provide high flux irradiation test capabilities similar to those of the HFIR, but the former has more irradiation channels than the latter does.

Japan has several high flux research reactors, among which the Japan Material Testing Reactor (JMTR) has the highest thermal power level (50 MW). The maximum neutron flux of the JMTR is approximately 4×10^{14} n cm^{-2} s^{-1} [8, 9]. The JMTR features a tank in a pool-type reactor with light water cooling. The JMTR reached criticality for the first time in March 1968 and was mainly applied to fuel and material irradiation tests for light water reactors, high-temperature gas-cooled reactors, and radioactive isotope production [10].

The high flux reactor (HFR) in Petten, the Netherlands, is also a poop-type test reactor with a thermal power of 45 MW [11, 12]. The HFR has been operating steadily since September 1960 and has been widely used in nuclear fuel irradiation tests and medical isotope production. The HFR has already reached its designed life, and its decommissioning is in the planning stage.

The Jules Horowitz Reactor (JHR) is now under construction at the Cadarache Research Center in the south of France, and the plan is for it to maintain fission research capacity in Europe after 2020. The JHR is also a tank pool-type reactor with a thermal power of 100 MW and can reach a high fast neutron flux level in the core (~10^{15} n cm^{-2} s^{-1}, $E\geq0.1$ MeV) and a high thermal flux level in the reflector (~4.5×0^{14} n cm^{-2} s^{-1}, $E\leq0.625$ eV) [13]. The JHR has been designed with high flexibility to satisfy the requirements of fuel or material irradiation tests and medical isotope production.

The SM-3 reactor in Russia is a pressurized water reactor with a thermal power of 100 MW, and the neutron flux in the irradiation channels can reach $(3–5)\times10^{15}$ n cm^{-2} s^{-1} [14]. The missions of SM-3, such as testing nuclear fuel and material irradiation and producing radioactive isotopes, are similar to those of other high flux research reactors.

China has three high flux research reactors in operation: the High Flux Engineering Test Reactor (HFETR) [15], the China Advanced Research Reactor (CARR) [16], and the China Mianyang Research Reactor (CMRR) [17]. The HFETR can provide the highest neutron flux level among the three research reactors.

The main parameters of these typical high flux reactors are listed in Table 1.

Table 1 Main parameters of typical high flux reactors worldwide

Parameters	ATR	HFIR	SM-3	JMTR	HFR	JHR	HFETR
Country	USA	USA	Russia	Japan	Netherlands	France	China
Design power (MWt)	250	100	100	50	45	100	125
Average power density (kW L^{-1})	1000	1930	1927	425	310	800	1000
Fuel element	Parallel curved plates, U_3O_8–Al	Involute curved fuel plates, U_3O_8–A1	Rod fuel element	Flat plates, U_3Si_2–Al	Flat plates, U_3Si_2–Al	Concentric curved fuel plates, U_3Si_2–Al	Concentric curved fuel plates, U_3Si_2–Al
Type	Tank	Tank	Pressure vessel	Tank	Tank	Tank	Tank
Status	Operational	Operational	Temporary shutdown	Temporary shutdown	Permanent shutdown	Under construction	Operational

As shown in Table 1, most high flux research reactors are pool-type tanks because the primary coolant system needs to be pressurized to increase the saturation temperature. This measure can avoid primary coolant boiling in the outlet. These high flux research reactors have adopted a compact core arrangement with plate-type fuel elements, whose average power densities are usually higher than those of commercial pressurized water reactors. The reactor core arrangements of several typical high flux research reactors are illustrated in Fig. 1 [4, 6, 12, 15]. The diameter and height of these high flux research reactor active cores are typically no longer than 1 m. The average power density is usually hundreds of kilowatts per liter. The features of high safety and high neutron flux cannot be achieved simultaneously in the early high flux research reactors. For example, the neutron flux of the HFIR is the highest in the USA, but the safety feature cannot fulfill current requirements. Therefore, high flux research reactors that can simultaneously fulfill multiple requirements are necessary for advancing the nuclear industry.

These high flux research reactors are the cornerstone in the development of nuclear technologies. As demonstrated, the missions of current high flux research reactors can generally be summarized as follows:

1. Conduct nuclear fuels and materials behavior research under real irradiation conditions.

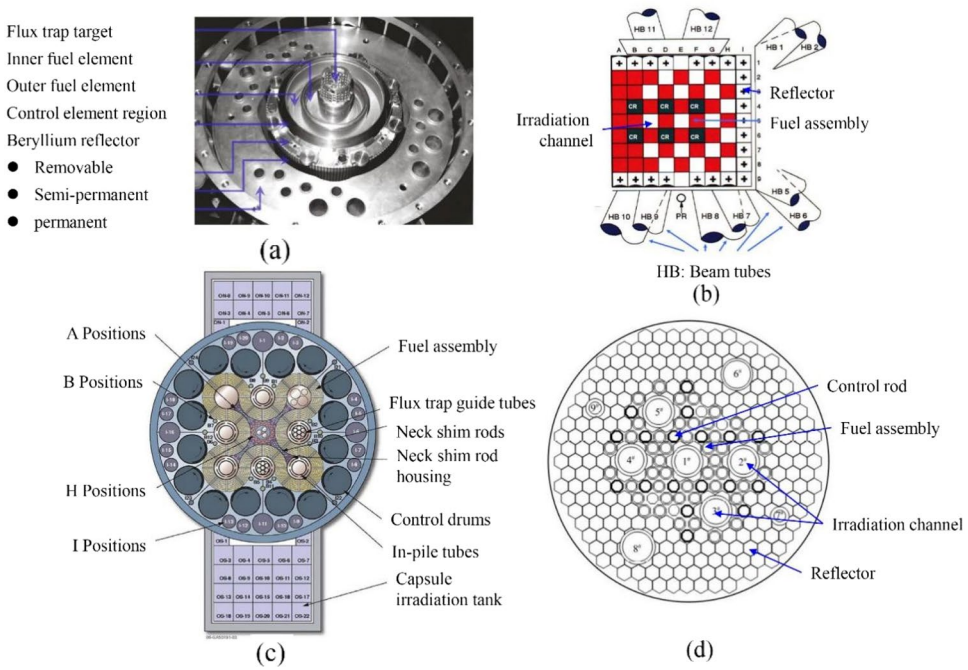

Fig. 1 (Color online) Reactor core cross-sectional schematics for several high flux reactors. **a** Cross-sectional view of HFIR core; **b** schematic of HFR core; **c** cross-sectional view of ATR core; **d** reactor core diagram of HFETR

2. Produce radioactive isotopes for medical and industrial purposes.
3. Conduct neutron scientific research, for example, neutron scattering, neutron imaging, and neutron activation.
4. Supply a platform to the nuclear industry for education and training for scientists, engineers, students, and companies.

China currently has three high flux research reactors, which do not satisfy the requirements of the nuclear industry and nuclear technology applications. Therefore, an innovative multi-mission high flux research reactor, as one of the national major scientific research infrastructures, is being designed by Tsinghua University. This paper mainly focuses on the characteristics and safety performance of this new multi-mission high flux research reactor designed by Tsinghua University (hereafter, MHFRR). The main design objectives of this MHFRR are as follows:

1. Both the average thermal and fast neutron flux will be higher than 1.5×10^{15} n cm^{-2} s^{-1} to satisfy the various irradiation and scientific missions.
2. The length of a single-fuel cycle must be longer than 25 days to reduce the frequency of refueling operations and improve the reactor economy.
3. The safety performance must satisfy the current nuclear safety requirements and standards of the National Nuclear Safety Administration.

In this paper, the second section introduces the general design of the MHFRR, including the design of the reactor core and thermal hydraulic. The third section analyzes the irradiation ability of the MHFRR. Some typical accidents that reflect the safety characteristics of the MHFRR will be analyzed in detail. The thermal hydraulic computational model of the MHFRR was simulated using RELAP5. The correlations for predicting the critical heat flux were written as a control component type card in the RELAP5 input files.

2 General design

2.1 Design of reactor core

As discussed, the purpose of high flux research reactors is to conduct various irradiation tests and neutron-related studies. Therefore, a high fast and thermal neutron flux is the key target of the core design. Some methods can be applied to improve the neutron flux, and the main methods are discussed as follows.

2.1.1 Methods of improving neutron flux

The goal of a commercial nuclear power plant is to generate electricity and make the output power as high as possible. However, high flux research reactors must have sufficient irradiation space and high thermal or fast neutron flux in the irradiation channels to promote safety and reduce costs. Without the restriction of output power and high efficiency, high power density can become the key factor in improving the neutron flux.

According to reactor physics, the neutron flux is related to the power density and fission cross section, which can be expressed by the following equation [18, 19]:

$$\phi = \frac{R_f}{\Sigma_f} = \frac{R_f}{N\cdot\sigma_f} \propto \frac{P_d}{N\cdot\sigma_f}, \tag{1}$$

where R_f is the fuel fission reaction rate, cm^{-3} s^{-1}; P_d is the average power density, W cm^{-3}; Σ_f is the macroscopic fission cross section, cm^{-1}; σ_f is the microscopic fission cross section, cm^2; N is the nuclide number density, cm^{-3}; and ϕ is the neutron flux, n cm^{-2} s^{-1}.

The aforementioned equations show that the neutron flux ϕ is directly proportional to the average power density P_d and inversely proportional to the macroscopic fission cross section Σ_f. Therefore, the following two methods can be considered to improve the neutron flux: improve the fuel power density and reduce the macroscopic fission cross section Σ_f.

The neutron flux can be effectively increased by improving the core power density. As shown in Table 1, the power density of current high flux research reactors is significantly higher than that of commercial pressurized water reactors. For example, the power density of HFIR or SM-3 is approximately 17 times that of the typical pressurized water reactor AP1000 [20]. For obtaining reactor criticality and increasing power densities simultaneously, highly enriched uranium fuel is usually required. However, a high power density also means a short continuous core operation time for the same fuel loading; thus, the length of the fuel cycle is usually only a few tens of days. For example, for the HFIR core, the neutron flux of the irradiation channel in the core center and the single length of the fuel cycle at different power densities are shown in Table 2. The maximum neutron flux with a power of 150 MW is approximately two times that with 85 MW, and the single-fuel cycle length is only 13.9 days when the power is 150 MW. Therefore, the neutron flux cannot be improved limitlessly by increasing the reactor power density.

As aforementioned, decreasing the average fission cross section can also improve the neutron flux, which can be realized by making the core area undermoderated and the energy spectrum hard. In this manner, the core area can reach a high fast neutron flux. Materials such as heavy water, beryllium, or graphite can be used as reflectors and arranged surround

Table 2 Maximum neutron flux in irradiation channel and cycle length of HFIR

Power (MW)	Maximum neutron flux (n cm^{-2} s^{-1})			Single cycle length (day)
	$E<0.625$ eV	$E>100$ eV	Total neutron flux	
85	2.30×10^{15}	2.20×10^{15}	4.64×10^{15}	24.6
100	2.71×10^{15}	2.59×10^{15}	5.46×10^{15}	20.9
120	3.25×10^{15}	3.11×10^{15}	6.55×10^{15}	17.4
150	4.06×10^{15}	3.88×10^{15}	8.19×10^{15}	13.9

Aforementioned parameters were calculated based on the cycle 400 input file for HFIR [21];
The maximum perturbed neutron flux is given in the table

the core. Thus, the fast neutrons that leak from the core are fully moderated in the reflector and mostly become thermal neutrons. Therefore, the thermal neutron flux in the reflector can reach a high level. By means of this design idea, the fast neutron irradiation channels are arranged in the core area, and the thermal neutron irradiation channels are arranged in the reflector area, which can realize the space separation of fast neutrons and thermal neutrons. This design is a typical "anti-neutron trap-type" core design.

2.1.2 Core design

The MHFRR is a pressure vessel-type research reactor with concentric fuel plate elements, heavy water as the coolant and moderator, and beryllium as the reflector, and the entire reactor pressure vessel is located in a light water pool. The core is composed of seven fuel assemblies and surrounded by a beryllium reflector, which provides efficient neutron moderation and reflection. The fuel assembly comprises a series of concentric regions. Each fuel plate contains fuel meat in the form of U_3Si_2–Al dispersion encapsulated in the aluminum alloy matrix. The fuel plate thickness is 2 mm. The fuel meat is 1 mm, and the outer cladding is 0.5 mm. The channel gap between the two plates of the inner fuel assemblies is 2 mm, and that of outer fuel assemblies is 4 mm. Six control drums are arranged in the reflector. The active core is compact: 50 cm high and an equivalent active diameter of approximately 60 cm. The in-core irradiation channel is in the center of the fuel assembly. In addition, irradiation channels are arranged in the beryllium reflector and outside the reactor for thermal neutron utility. Horizontal neutron beam channels can also be set for neutron scattering experiments. The MHFRR can be used to support, for example, radioactive isotope production, fuel and material irradiation tests, cold and thermal neutron scattering experiments, and neutron activation analysis. The main design parameters of the MHFRR are shown in Table 3. The core cross section is shown in Figs. 2 and 3.

This MHFRR adopts heavy water as the coolant because of its excellent moderated performance. The core fuel zone is radially divided into one central fuel zone and six peripheral fuel zones. The inner fuel zone is 90 wt% high-enriched uranium, and the outer six fuel zones are 20 wt% low-enriched uranium. Therefore, the fuel content per unit volume in the central fuel zone is much higher than that in the peripheral fuel zone, and the difference in the water-to-uranium ratio between these two regions could reach more than 20 times. Thus, the neutron energy spectra are very different. Figure 4 shows the normalized neutron energy spectra of the inner and outer irradiation channels for the MHFRR. The inner irradiation channel is a fast neutron ($E>100$ eV) spectrum area, and the outer irradiation channel is a thermal neutron ($E<1$ eV) spectrum area. Thus, the space separation of fast and thermal neutrons in the active region of the core is realized. In practical applications, only fast neutrons or thermal neutrons in the irradiation channel are typically used, and obtaining high fast and thermal neutron fluxes at the same location is unnecessary. If both fast and thermal neutrons reach a high neutron flux in the same irradiation channel, the total neutron flux at this location would be too large, which requires the surrounding fuel to reach a very high power density. The space separation of fast and thermal neutrons in the active region of the core can significantly reduce the average power density and increase the number and volume of irradiation channels. In addition, the power density in the central fuel area is significantly higher than that in the peripheral fuel area, which makes fission neutrons concentrate in the central fuel region. Taking full advantage of the long average free path length of neutrons in heavy water, fast neutrons in the central fuel area can enter the central channel, and most of the leaked neutrons can also enter the irradiation channel around the core. This design increases the number of fission neutrons to reach the irradiation channel and improves their utilization rate of fission neutrons.

With the characteristics of a long diffusion length and a large leakage of heavy water, fission neutrons in the core would leak into the beryllium reflector. Therefore, irradiation channels can also be set in the reflector. In order to avoid the power shape distortion caused by the insertion of the control rod, the control requirements can be fulfilled only by the control drum set in the reflector, which can greatly reduce the maximum power density and improve safety.

Table 3 Main design parameters of the MHFRR at steady-state condition

Parameters		Value
Thermal power (MW)		70
Pressure of the primary coolant system (MPa)		2
Reactor core height (cm)		50
Equivalent diameter of reactor core active region (cm)		60.0
Reflector material/thickness (cm)		Be/30
Radius of inner/outer fuel assembly (cm)		10.5/10.5
Radius of inner/outer irradiation channel (cm)		5.5/4.0
Average coolant temperature of reactor inlet (°C)		50
Average coolant temperature of reactor outlet (°C)		60
Coolant flow rate between fuel plates ($m \cdot s^{-1}$)		10.0
Maximum temperature of cladding surface (°C)		178
Minimum departure from nucleate boiling ratio (MDNBR)		3.2
Multiplication factor (k_{eff}) with all the control drums out/in		1.1693/0.8396
Moderator/fuel temperature coefficient ($pcm \cdot K^{-1}$)		–17.6/–1.79
Initial uranium loading/^{235}U loading (kg)		67/12.4
The length of fuel cycle (d)		27.5
Average power density ($MW\ m^{-3}$)		680
Average power density of inner/outer fuel region ($MW\ m^{-3}$)		1551/567
Maximum surface heat flux ($MW\ m^{-2}$)		3.5
The average value of neutron flux in the center channel ($n\ cm^{-2}\ s^{-1}$)	Thermal ($E < 1$ eV)	2.0×10^{15}
	Fast ($E > 100$ eV)	2.9×10^{15}

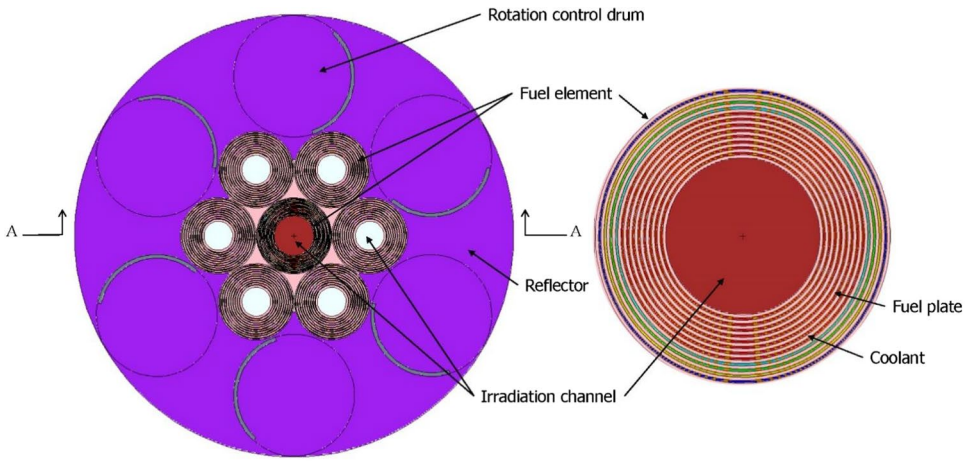

Fig. 2 (Color online) Schematic cross section of the reactor core

2.2 Design of thermal hydraulic

As shown in Fig. 5, the primary coolant system has four loops under operation with one-loop spare set. Four primary coolant pumps, connected in parallel, circulate 2000 kg s^{-1} under nominal conditions. The pressurized water enters the reactor vessel, approximately 50% of the coolant flows through the fuel elements, and the remainder is used to cool the reactor internals and auxiliary experimental facilities. The basic premise of thermal hydraulic analysis is that the maximum temperature of the fuel plate cladding surface should be no higher than the temperature design limit and no nucleate boiling will commence on the plate surface. In order to achieve these goals, some design concepts are adopted in the MHFRR.

2.2.1 Plate-type fuels

Because of the high reactor power density and large fuel loading capacity, the plate-type fuel element is usually used to efficiently transfer the heat generated by the fuel. As Fig. 6 shows, the uranium-containing fuel is dispersed in the aluminum matrix, and the fuel plates can be machined into different shapes, such as involute plates, flat plates, folding

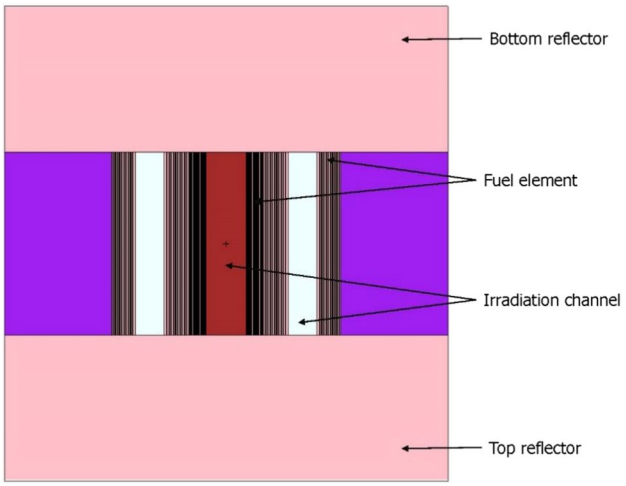

Fig. 3 (Color online) Schematic of the longitudinal section of the reactor core

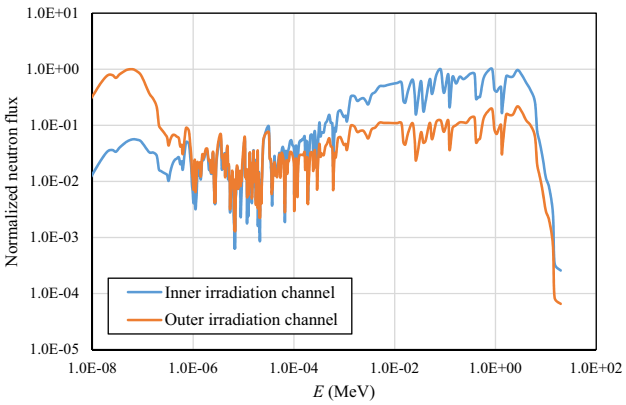

Fig. 4 (Color online) Normalized neutron energy spectrum of the irradiation channel

plate types, and concentric circular rings [22]. A thin fuel plate can have a larger heat transfer area with the same volume of fuel than other types, but the temperature limit of this thin fuel plate is relatively low. Usually, the temperature design limit of the fuel plate cladding surface is not more than 250 °C to prevent cladding blisters, and the maximum temperature of the fuel meat is not more than 500 °C. The temperature design limit of the cladding surface limits the maximum power density. As shown in Fig. 2, the fuel plates of the MHFRR are similar to those of the HFETR and ATR, and the temperature design limit is 234 °C according to the HFETR [15]. The maximum temperature of the cladding surface at the nominal operating condition is only 178 °C, which still has a margin of approximately 56 °C.

2.2.2 Pressurized coolant with high velocity

Owing to the high power density, the enthalpy rise of the coolant is relatively large. In order to prevent coolant boiling at the outlet, methods such as reducing the coolant temperature at the inlet or increasing the coolant saturation temperature by increasing the pressure of the primary coolant system are typically adopted. Therefore, current high flux research reactors are mostly pressurized, and the inlet temperature of the coolant is significantly lower than that of commercial power plants. The pressure of the primary coolant system is 2 MPa, and the reactor coolant inlet temperature is 50 °C for the MHFRR. In addition, owing to the high power density, the coolant flow velocity between the thin plates is usually relatively high to prevent the departure from nucleate boiling (DNB). The coolant velocity through fuel is usually approximately 10 m s^{-1}. For example, the mean velocity through fuel is 12 m s^{-1} for the HFIR [4], 14 m s^{-1} for the ATR [5], 15 m s^{-1} for the JHR [13], and 10 m s^{-1} for the HFETR [15]

Fig. 5 (Color online) Primary coolant system of the MHFRR

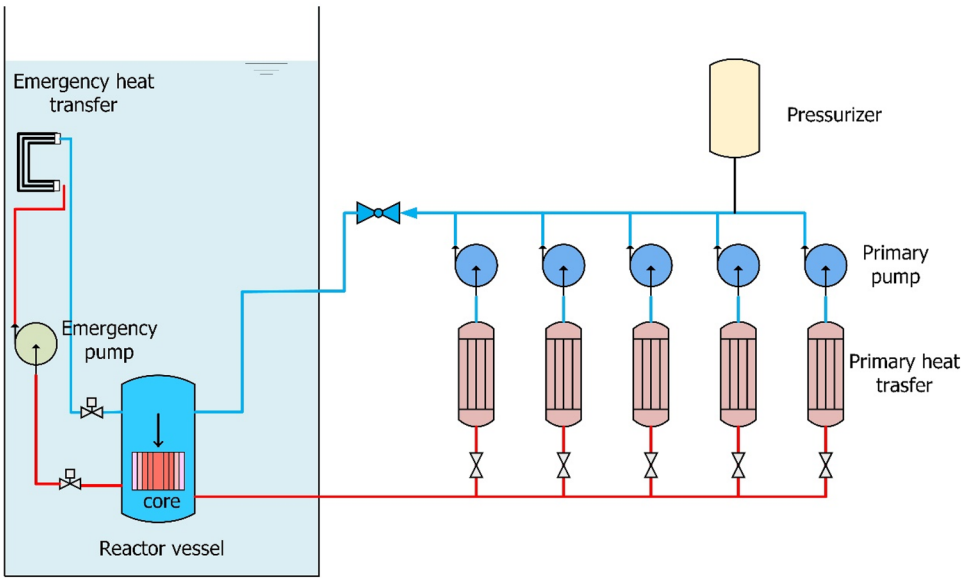

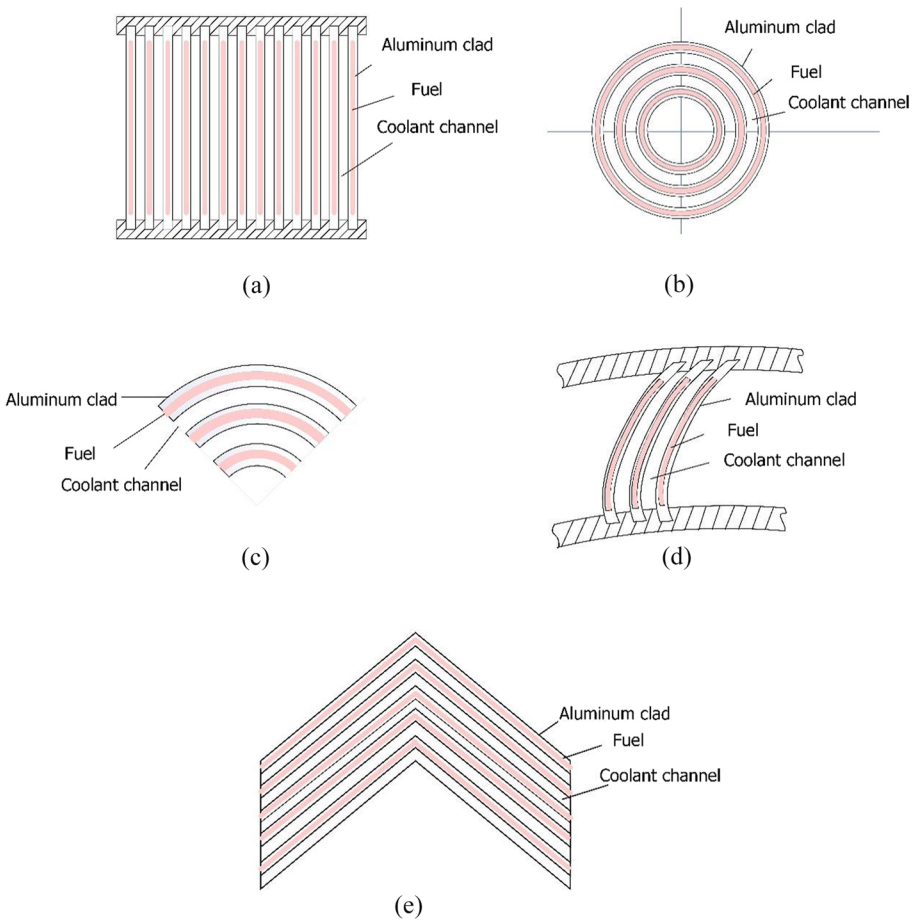

Fig. 6 (Color online) Schematic of plate fuel elements used in the research reactors. **a** The flat fuel plates in JMTR and JRRS; **b** the concentric fuel plates in HFETR; **c** the cylindrical fuel plates in ATR; **d** the involute fuel plates in HFIR and ANSR; and **e** the folded fuel plates

but only 4.8 m s^{-1} for the AP1000 [20]. High velocity may cause plate vibration and result in high requirements for the structural performance of fuel plates. Therefore, the design average coolant velocity between fuel plates is 10 m s^{-1} for the MHFRR.

2.2.3 Downward flow in the reactor core

Compared with commercial nuclear power plants, high flux research reactors have a shorter fuel cycle, usually tens of days. Frequent refueling operation means that the top cover of the tank or vessel needs to be opened frequently. For easy refueling operation, the structure of the top of the reactor core needs to be as simple as possible, and the fuel assemblies are usually simply placed on the support component. If the coolant flows from bottom to top through the core, it may wash away the fuel assemblies; thus, the coolant of most high flux reactors flows from top to bottom through the core. Therefore, the flow direction is also designed to be downward in the reactor core for this MHFRR.

However, this downward flow may create a new problem: In the case of a station blackout (SBO) accident, the forced circulation of the residual heat removal system is stopped when the emergency accumulator battery stops the power supply. A natural circulation between the reactor core and the emergency heat exchanger will occur owing to the temperature difference. This natural circulation flows from bottom to top in the core, contrary to the forced flow direction in normal operation. When the forced flow stops and decay heat release remains in the core, a transition process from forced flow to natural circulation occurs, called "flow inversion." This situation inevitably occurs after an SBO accident if the forced flow direction is from top to bottom in the core. Therefore, the decay heat and natural circulation capacity should be considered in reactor design. A detailed analysis of natural circulation capacity is given in Sect. 4.2.

3 Irradiation ability analysis

The primary role of the MHFRR is to conduct irradiation tests of advanced fuels and structural materials and produce radioactive isotopes. Therefore, irradiation ability is an important technical index for high flux research reactors. The HFETR is the only research reactor that can supply neutron flux with a 10^{15} n cm^{-2} s^{-1} level and has the best

irradiation ability among those in China. Therefore, this section presents a detailed irradiation ability comparison with HFETR on the premise of reactor safety.

The safety characteristics of a high flux research reactor can be reflected by safety margins. The safety margin of the high flux research reactor is the difference or the ratio between the limiting threshold value and the actual value. Exceeding the limiting threshold value leads to the failure of a component or system in the reactor [23]. The safety margins of these research reactors include the maximum temperature of the cladding surface and the minimum departure of the nucleate boiling ratio (MDNBR). The safety margins of the HFETR and MHFRR at steady-state conditions are shown in Fig. 7.

The irradiation ability is a comprehensive reflection of the neutron flux, irradiation space, and irradiation time provided by the high flux research reactor. The irradiation time is dependent on the operation time of the research reactor. For the current core design, a large irradiation volume and high neutron flux are required. The irradiation ability can be calculated using Eqs. (2) and (3) [24]:

$$Q_{\mathrm{y}} = 86400 t \phi V, \tag{2}$$

$$Q_{\mathrm{d}} = 86400 \phi V, \tag{3}$$

where Q_{y} is the irradiation ability per year, cm·a^{-1}; Q_{d} is the irradiation ability per day, cm d^{-1}; ϕ is the average neutron flux at design power, n cm^{-2} s^{-1}; and V is the volume of the irradiation space, cm^3. t is the irradiation time, d. A comparison of the irradiation ability of the HFETR and MHFRR is shown in Table 4.

As shown in Fig. 7, both the safety margin of the maximum temperature of the cladding surface and the MDNBR of the MHFRR are larger than those of the HFETR under steady-state conditions. In other words, the MHFRR has better safety performance than the HFETR. Further, as shown in Table 4, the neutron flux and irradiation ability of the MHFRR are better than those of the HFETR. In conclusion, the MHFRR has an excellent irradiation ability and sufficient safety margins.

Table 4 Irradiation ability comparison of HFETR and MHFRR

Parameters	HFETR	MHFRR
Design power (MW)	125	70
Fast neutron flux (n cm^{-2} s^{-1})	1.7×10^{15} (max value)	2.9×10^{15} (mean value)
Thermal neutron flux (n cm^{-2} s^{-1})	6.2×10^{14} (max value)	2.0×10^{15} (mean value)
Equivalent fuel power days	180	280
Irradiation ability per day (cm d^{-1})	1.806×10^{25}	2.11×10^{25}
Irradiation ability per day (cm a^{-1})	3.251×10^{27}	5.90×10^{27}

4 Safety analysis

In the current design of the MHFRR, the pressure of the primary coolant system is 2 MPa, the coolant velocity between the channels of fuel plates is 10 m s^{-1}, and the coolant inlet temperature is 50 °C. Four loops are in operation, and one loop is in a standby state under normal operation. For ensuring the removal of reactor decay heat, there is also a residual heat removal system. The residual heat removal system comprises two emergency pumps and two emergency heat exchangers. Based on this preliminary design, the temperature design limit of the cladding surface to prevent cladding blister, the MDNBR, and the onset of nucleate boiling to prevent heat transfer deterioration are the main safety criteria, specifically,

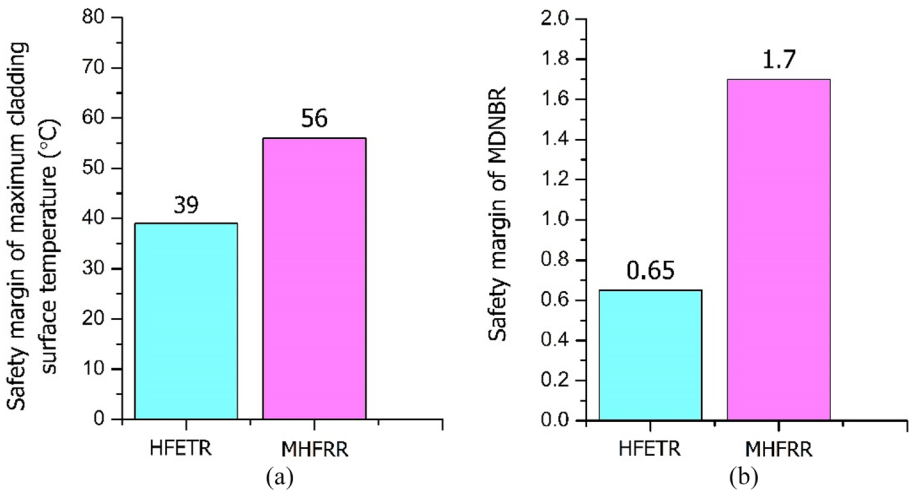

Fig. 7 (Color online) Safety margins at steady-state condition. **a** Safety margin of maximum cladding surface temperature; **b** safety margin of MDNBR

1. The maximum temperature of cladding surface is $T_{c,max} < 234$ °C.
2. The minimum DNB ratio is (MDNBR) > 1.5.
3. The wall temperature T_w is less than the onset of nucleate boiling temperature T_{ONB}, namely, $T_{ONB} > T_w$.

Under accident conditions, when all three safety criteria are satisfied, the safety performance of the MHFRR can be acceptable. In order to verify the three safety criteria of the MHFRR, typical accidents such as SBO accidents, loss of coolant accidents (LOCAs), and reactivity accidents have been analyzed by RELAP5/MOD3.2. A nodalization diagram of the primary coolant and heat removal systems is shown in Fig. 8. The critical heat flux (CHF) model adopts the correlations of Sudo [25, 26]. The Bergles–Rohsenow correlation was adopted to predict the onset of nucleate boiling (ONB) [27]. The heat transfer correlation uses the Dittus–Boelter correlation [28].

CHF correlations:

$$q^*_{CHF,1} = 0.005|G^*|^{0.611}\left(1 + \frac{5000}{|G^*|}\Delta T^*_{sub,o}\right) \tag{4}$$

$$q^*_{CHF,2} = \frac{A}{A_H}\Delta T^*_{sub,i}|G^*| \tag{5}$$

$$q^*_{CHF,3} = 0.7\frac{A}{A_H} \times \frac{\sqrt{W/\lambda}}{\left[1 + \left(\rho_g/\rho_l\right)^{0.25}\right]^2} \tag{6}$$

ONB correlation:

$$q_{ONB} = 1.798 \times 10^{-3} P^{1.156}\left[1.8\left(T_w - T_s\right)\right]^{2.828/P^{0.0234}} \tag{7}$$

Heat transfer correlation:

$$Nu = 0.023 Re^{0.8} Pr^{0.4} \tag{8}$$

4.1 SBO accident analysis

According to the analysis of existing high flux research reactors in China, from 1981 to the end of 1995, more than 40 unplanned shutdowns were caused by the loss of external power supply [29]. Therefore, to ensure the safety of the MHFRR, SBO accidents must be analyzed in detail. The results of the SBO accident analysis for the MHFRR are shown in Fig. 9.

An SBO accident is supposed to occur at 0 s, and the emergency shutdown signal will be delayed for 2 s after an 80% low flow rate signal is detected (2 s for the delay time is conservative). The results of the SBO accident analysis show that the maximum temperature of the cladding surface is 196.7 °C, which is lower than the temperature limit of 234 °C and still has a margin of 37 °C. The coolant outlet temperature of the hot channel is approximately 107.1 °C, and the corresponding saturation temperature is approximately 212 °C. Thus, no coolant boiling phenomenon occurs in the core, and the margin remains 105 °C. As shown in Fig. 9, there are two danger points in the entire process after reactor shutdown. The first point appears at 3 s, and the MDNBR is 2.32, which occurs just before the emergency reactor shutdown signal is issued. In this period, the coolant flow through the core begins to decrease, the reactor power

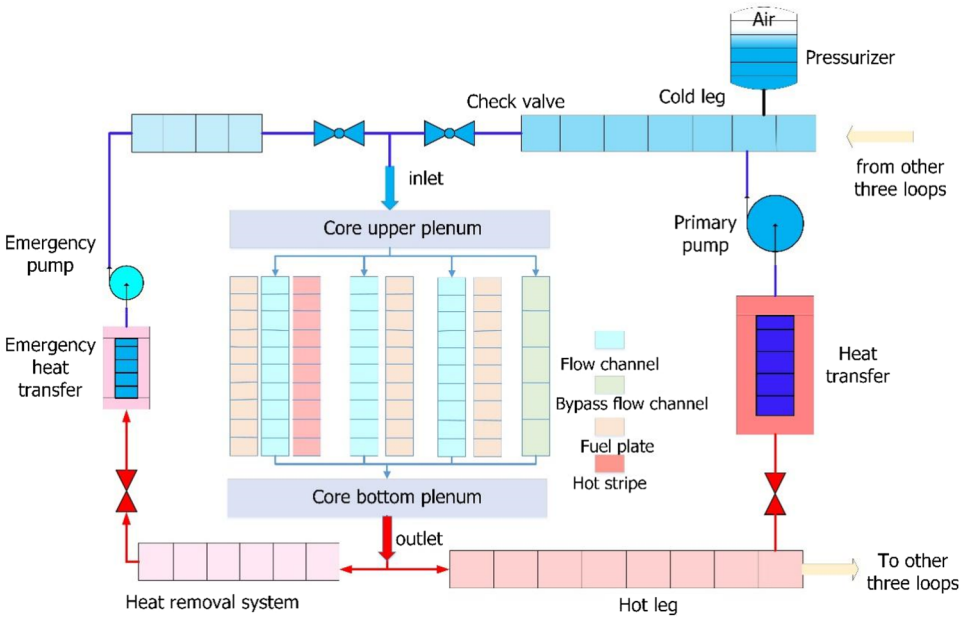

Fig. 8 (Color online) RELAP5 nodalization diagram of the primary coolant system and the heat removal system

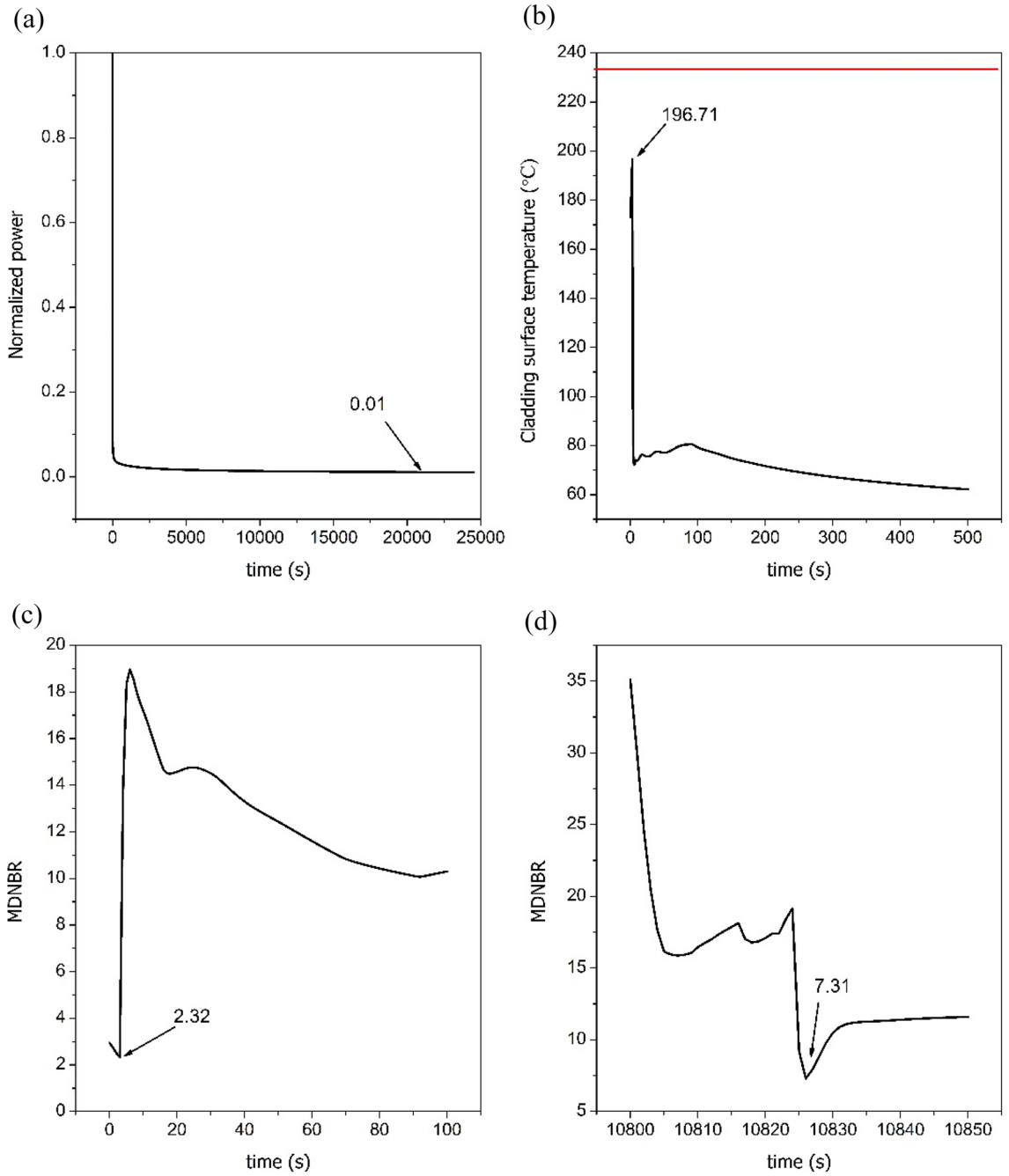

Fig. 9 Results of SBO accident for MHFRR. **a** Normalized power versus time, **b** cladding surface temperature versus time, **c** MDNBR versus time in beginning period, and **d** MDNBR versus time after 10,800 s

remains at nearly full power, the cooling of the fuel is insufficient, and the fuel temperature increases. After the reactor shutdown signal is triggered, the reactor power decreases rapidly, and the MDNBR begins to increase. The second danger point occurs at the moment of "flow inversion" after the emergency pump stops at 10,800 s. The MDNBR decreases rapidly, and the second minimum point, 7.31, of the MDNBR appears at 10,826 s. The coolant velocity at this moment is zero, and subsequently, the coolant between the fuel plates begins to flow upward. This phenomenon is "flow inversion." After the natural circulation between the emergency heat exchanger and reactor core is established, the MDNBR is increased.

The aforementioned analysis of SBO accidents shows that the safety margins of the MDNBR and maximum temperature of the cladding surface remain sufficient.

As shown in Table 5, the safety margin of the MHFRR remains larger than that of the other three high flux research reactors in China [30]. The safety margin of the maximum temperature of the cladding surface for the CMRR is large because of the low coolant inlet temperature. However, for the MHFRR, the advanced design concept of the space separation of fast and thermal neutrons in the active core region can improve the neutron flux and increase the safety margin simultaneously.

4.2 Analysis of passive residual heat removal capacity

When the emergency accumulator battery stops supplying power to the emergency pump, the decay heat still has approximately 1% of the nominal thermal power. In order to remove the residual heat, the reactor must have a certain natural circulation capacity when the emergency pump stops working. The reactor vessel is placed in the reactor pool at normal temperature and pressure. The emergency heat exchanger is in another pool, and the heat of the pool can be transferred to the outside air by a passive mechanism. A natural circulation system is used because of the temperature difference between the reactor core and the emergency heat exchanger. According to the current design, the pool temperature is 25 °C, the average core fluid temperature is approximately 35 °C, and the height difference between the core and the emergency heat exchanger is approximately 12 m. The driving head ΔP_{d} of the natural circulation should be equal to the sum of the elevation pressure drops ΔP_{el}:

$$\Delta P_{\mathrm{d}} = \oint \Delta P_{\mathrm{el}} = \int_0^L \left[\rho_{\mathrm{pool}} - \rho_{\mathrm{core}}\left(T_{\mathrm{f}}\right)\right] g \mathrm{d}z. \tag{9}$$

ΔP_{d} can be calculated as follows:

$$\Delta P_{\mathrm{d}} = 354.0 \text{ Pa}. \tag{10}$$

Table 5 Safety margin of high flux research reactors in SBO accident

Parameters	MHFRR	HFETR	CARR	CMRR
Thermal power (MW)	70	125	56.4	20
Safety margin of MDNBR	0.82	0.65	0.36	0.22
Safety margin of maximum temperature of cladding surface (°C)	37.3	39	11	51

The MDNBR and maximum temperature of the cladding surface of the HFETR are obtained from analysis under steady-state conditions. The safety margin in an SBO accident will be less than 0.65–39 °C

The relationship between ΔP_{d} and the mass flow rate of natural circulation is as follows:

$$\Delta P_{\mathrm{d}} = \sum_i \left(f \frac{L}{\mathrm{De}} \frac{1}{2\overline{\rho} A^2} + \xi \frac{1}{2\overline{\rho} A^2} \right) \times \dot{m}^2 = \frac{\xi_{\mathrm{tot}}}{2\overline{\rho} A^2} \times \dot{m}^2. \tag{11}$$

According to the design of the entire natural circulation loop, the total resistance can be estimated:

$$\frac{\xi_{\mathrm{tot}}}{2\overline{\rho} A^2} \approx 1.35 \text{ kg}^{-1} \text{ m}^{-1}. \tag{12}$$

The natural circulation flow rate can be calculated to be approximately 16.2 kg s^{-1} from Eqs. (9) to (12). The temperature difference of the coolant between the inlet and outlet was approximately 20 °C. Thus, the decay heat that can be removed by natural circulation can be approximated:

$$\begin{aligned} Q_{\mathrm{nc}} &= C_{\mathrm{p}} \dot{m} \Delta T = 4200 \text{J kg}^{-1} \, ^{\circ}\text{C}^{-1} \times 16.2 \text{ kg s}^{-1} \times 20 \, ^{\circ}\text{C} \\ &= 1.36 \text{ MW}. \end{aligned} \tag{13}$$

The decay heat when the emergency accumulator battery stops supplying power is approximately 0.93 MW. Thus, the natural circulation can remove the residual heat owing to the preliminary design of the MHFRR.

4.3 LOCA analysis

The LOCA is a typical accident type of pressurized water reactors. When a break occurs in the primary coolant system, the pressure of the system decreases, and the coolant is rapidly discharged from the break. The fuel elements may melt if the reactor core cannot be cooled in a timely manner. Owing to the compact core design and the high heat flux of fuel elements in high flux research reactors, relying on forced circulation by the residual heat removal system is necessary to remove the residual heat early in the accident. At the beginning of the LOCA, water is replenished to the core through the injection tanks to delay the pressure drop of the primary coolant system. The reactor pressure vessel was immersed in the reactor pool, and a check valve was arranged between the reactor pool and the reactor pressure vessel. When the pressure of the primary coolant system drops to the set pressure of the valve, the water in the reactor pool can be injected into the reactor pressure vessel to ensure that the reactor core is immersed. After natural circulation is established, the residual heat of the core can be carried away.

The results of the analysis of the positions and sizes of the breaks are shown in Table 6.

As shown in Table 6, both the MDNBR and the margin between wall temperature and ONB temperature decrease as the break size increases. In other words, the larger the break size, the smaller the safety margin. Under the current design,

Table 6 Results of LOCA analysis

Break position	Results	2 in	3 in	4 in	5 in	6 in
Primary pump outlet	MDNBR	2.80	2.69	2.56	2.16	2.04
	$T_{ONB} - T_w$ (°C)	59.7	54.2	46.8	22.2	7.3
Primary pump inlet	MDNBR	2.81	2.75	2.45	2.37	2.30
	$T_{ONB} - T_w$ (°C)	60.6	57	40.8	35.6	31.4
Primary heat transfer inlet	MDNBR	2.82	2.75	2.69	2.61	2.36
	$T_{ONB} - T_w$ (°C)	60.8	56.4	52.6	47.8	28.6
Hot leg	MDNBR	2.82	2.74	2.59	2.43	2.26
	$T_{ONB} - T_w$ (°C)	60.8	56.1	44.4	34.6	27.2
Cold let	MDNBR	2.80	2.78	2.63	2.29	2.09
	$T_{ONB} - T_w$ (°C)	60.5	57.5	49.9	27.9	13.3

the integrity of the core can be guaranteed in the event of a break below six at any location.

The coolant leaks too much from the reactor core, and forced circulation cannot be maintained with the double-ended guillotine break of the primary pump outlet. The fuel elements may melt if the coolant cannot be injected into the core in a timely manner. Therefore, further evaluation of the compensation capacity of the accumulator is required to ensure stable forced circulation. For the double-ended guillotine break of the cold leg or hot leg accidents, the loss of coolant is increased, the phenomenon change is significant, and the integrity of the core cannot be maintained. When the pressure of the primary loop is too low, air enters the break, which affects the heat transfer of the core and the operation of the emergency pump, posing a threat to fuel element integrity. Therefore, preventing the pressure of the primary circuit from decreasing too low after the LOCA is important. Increasing the back pressure of the check valve between the reactor pool and the pressure vessel may be a feasible compensation measure, and the feasibility needs to be analyzed in detail in further research.

4.4 Reactivity accident

In order to avoid distortion of axial power, the MHFRR uses six control drums to adjust reactivity. Misoperation, a failure of the reactor regulation system, or a failure of the control drum system may cause the control drum to rotate out. Positive reactivity is introduced if the control drum rotates from the critical position, which leads to an increase in reactor power and fuel temperature. The mismatch of the reactor power and primary coolant flow rate may result in the maximum surface temperature of the fuel cladding exceeding the temperature limit and the MDNBR being lower than the safety criteria. Figure 10 shows the reactivity value curve of the single control drum. According to the curve of the reactivity value for the control drum, the simulation results when the control drum is rotated out from the critical position under full power operation are shown in Fig. 11.

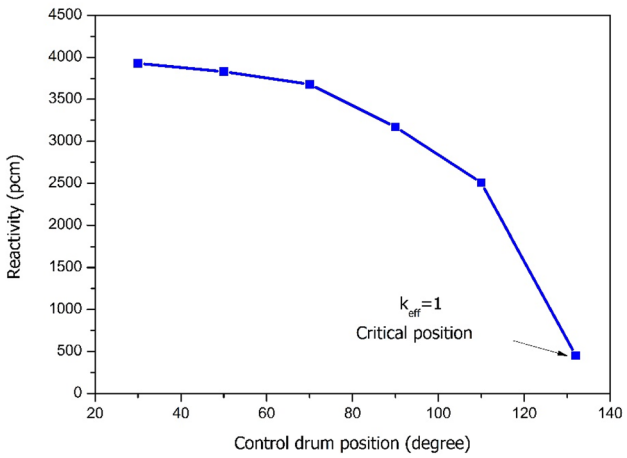

Fig. 10 Reactivity value curve of the single control drum

The simulation results were obtained under the assumption that the control drum can return to its original position, which is equivalent to introducing step positive reactivity. Additionally, a more conservative assumption is adopted, that is, no other protective measures are implemented except to make the control drum rotate to its original position.

The analysis results show that when the introduced positive reactivity is lower than 280 pcm (corresponding to the control drum rotation of 3°), the maximum temperature of the fuel cladding surface is 230.4 °C, which is lower than the temperature limit of 234 °C; the minimum value of DNBR is 1.73, which is higher than the limit value of 1.5; and the minimum temperature difference between the wall temperature and ONB temperature is 5.3 °C. The maximum temperature of the fuel cladding surface, the MDNBR, and the ONB temperature satisfy the requirements of the safety criteria. Moreover, the rotation speed of the control drum can be controlled to 0.1° s^{-1}. Three degrees require 30 s, which is sufficient for the protection systems to implement.

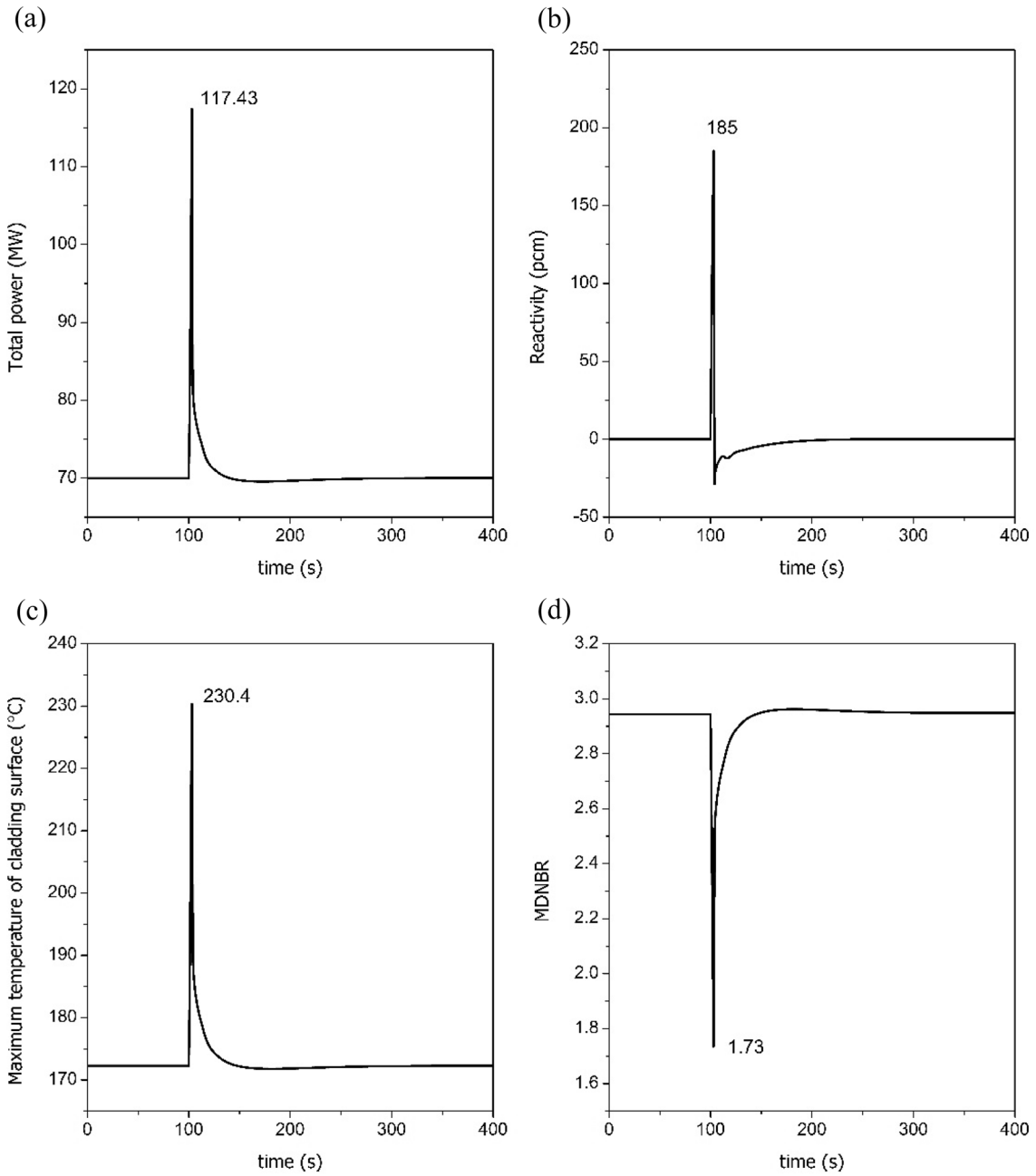

Fig. 11 Results of the control drum rotating out from the critical position under full power operation. **a** Total power versus time, **b** reactivity versus time, **c** maximum temperature of cladding surface versus time, and **d** MDNBR versus time

These results were obtained under the conservative assumption that no protective actions were implemented. Notably, once the power level reaches a certain level, various protective signals are triggered, and the reactor automatically implements protective measures, such as reactor shutdown. In this case, the consequences will be much lighter than those aforementioned, and the safety margins will be sufficient.

5 Conclusion

In conclusion, the MHFRR is designed as a vessel in a pool-type high flux research reactor with concentric fuel plate elements. The primary coolant system is 2 MPa to avoid coolant boiling in the reactor core. Heavy water was adopted as the coolant and moderator, and beryllium was used as the reflector. The average values of thermal and fast neutron flux in the irradiation channels are above 2.0×10^{15} n cm^{-2} s^{-1}.

This high neutron flux can fulfill the needs of most scientific research and medical and industrial isotope production.

Moreover, the space separation of fast and thermal neutrons can reduce the total neutron demand of each region. In this manner, the average power density can be greatly reduced, and the number and volume of irradiation channels can be increased. The design of a high neutron flux trap by optimizing the arrangement of heavy water and beryllium makes the utilization of fuel effective. Control drums are adopted to adjust the reactivity, which avoids power shape distortion and improves safety features. Based on these design principles, the irradiation ability and safety margins are significantly improved.

Furthermore, according to the accident analysis of the SBO accident, LOCA, and reactivity analysis, the maximum temperature of the fuel cladding surface, the MDNBR, and the ONB temperature can satisfy the requirements of the current safety criteria. These analysis results further prove the safety performance of the MHFRR. In addition, owing to the rich construction experience of pressurized water reactors, engineering the construction of MHFRR is less difficult and highly feasible.

Author contributions All authors contributed to the study conception and design. Material preparation, data collection, and analysis were performed by Wei Xu, Jian Li, Heng Xie, Zhi-Hong Liu, Jing Zhao, Fei Xie, and Lei Shi. The first draft of the manuscript was written by Wei Xu, and all authors commented on previous versions of the manuscript. All authors read and approved the final manuscript.

Data availability The data that support the findings of this study are openly available in Science Data Bank at https://doi.org/10.57760/sciencedb.j00186.00045 and http://resolve.pid21.cn/31253.11.sciencedb.j00186.00045.

References

1. L. Chen, R. Yan, X.Z. Kang et al., Study on the production characteristics of ^{131}I and ^{90}Sr isotopes in a molten salt reactor. Nucl. Sci. Tech. **32**, 33 (2021). https://doi.org/10.1007/s41365-021-00867-1
2. Z.Y. Zhang, Y.J. Dong, Q. Shi et al., 600-MWe high-temperature gas-cooled reactor nuclear power plant HTR-PM600. Nucl. Sci. Tech. **33**, 101 (2022). https://doi.org/10.1007/s41365-022-01089-9
3. B.R. Betzler, D. Chandler, E.E. Davidson et al., High-fidelity modeling and simulation for a high flux isotope reactor low-enriched uranium core design. Nucl. Sci. Eng. **187**(1), 81–99 (2017). https://doi.org/10.1080/00295639.2017.1292090
4. D. Chandler, C.D. Bryan, High flux isotope reactor (HFIR). Enc. Nucl. Eng. **4**, 64–73 (2021). https://doi.org/10.1016/B978-0-12-819725-7.00051-9
5. D.R. Deboisblanc, S. Cohen, Safety analysis report advanced test reactor, Vol 1 of 2. USA: atomic energy commission. IDO-17021. (1965). https://doi.org/10.2172/4495135
6. F.M. Marshall. T.R. Allen, J.B. Benson et al., Advanced test reactor: a national scientific user facility. In Proceedings of the 16th International Conference on Nuclear Engineering. Orlando, Florida. May 11–15, (2008). pp. 367–372. https://doi.org/10.1115/ICONE16-48426
7. J. Benson, J. Cole, J. Jackson et al., Operational philosophy for the advanced test reactor national scientific user facility. In USA: Idaho National Laboratory, INL/EXT-09–16332, (2013). Doi: https://doi.org/10.2172/1072393
8. M. Ishihara, H. Kawamura, M. Niimi et al., Refurbishment status and future program of japan materials testing reactor (JMTR). In Proceedings of 12th International Group on Research Reactors (12th IGORR), (2009). p.10
9. N. Takemoto, N. Sugaya, K. Ohtsuka K et al., Simulator for materials testing reactors. Japan: Japan atomic energy agency, JAEA-Technology 2013–013, (2013)
10. Y. Inaba, K. Iimura, J. Hosokawa et al., Status of development on Mo-99 production technologies in JMTR. IEEE T. Nucl. Sci. **58**(3), 1151–1158 (2011). https://doi.org/10.1109/tns.2011.2144620
11. L. Stefanini, F.H.E. de Haan-de Wilde, J.F. Offerein, High flux reactor continued safe operation: time limited ageing analyses. In Proceedings of the Vol 8: Operations, Applications, and Components. Virtual, Online. August 3, (2020). V008T08A010. ASME. https://doi.org/10.1115/PVP2020-21032
12. N.A. Hanan, J.R. Deen, J.E. Matos, Neutronic feasibility studies for LEU conversion of the HFR Petten Reactor. In 23rd International Meeting on Reduced Enrichment for Research and Test Reactors (RERTR), Las Vegas, NV (US). Argonne National Laboratory, (2000)
13. R. Pegonen, S. Bourdon, C. Gonnier et al., A review of the current thermal-hydraulic modeling of the Jules Horowitz Reactor: a loss of flow accident analysis. Nucl. Eng. Des. **280**, 294–304 (2014). https://doi.org/10.1016/j.nucengdes.2014.09.019
14. V.A. Tsykanov, A.V. Klinov, V.A. Starkov et al., SM reactor core modification solving materials-science problems. Atom. Energy. **93**, 713–717 (2002). https://doi.org/10.1023/A:1021763815423
15. C.X. Xu, Y.M. Zhou, J.H. Qian et al., High flux engineering test reactor. Nucl. Power Eng. **2**(03), 130–144 (1981). (**in Chinese**)
16. G.H. Su, W.X. Tian, S.Z. Qiu et al., Development of steady thermal-hydraulic analysis code for China advanced research reactor. At. Energy Sci. Technol. **40**(1), 51–56 (2006). https://doi.org/10.7538/yzk.2006.40.01.0051 (in Chinese)
17. B. Hu, S.M. Guo, G.B. Wang et al., Simulation of typical accidents in fuel test loop of CMRR. High Power Laser Part. Beams **31**, 096001 (2019). https://doi.org/10.11884/HPLPB201931.190023 (in Chinese)
18. W.M. Stacey, *Nuclear reactor physics* (Wiley, New York, 2018)
19. E.E. Lewis, *Fundamentals of nuclear reactor physics* (Elsevier, Amsterdam, 2008)
20. C.G. Lin, *Passive Safety Advanced Nuclear Power Plant AP1000* (Atomic Energy Press, 2008)
21. G. Ilas, D. Chandler, B.J. Ade et al., Modeling and simulations for the high flux isotope reactor cycle 400. USA: Oak Ridge National Lab. ORNL/TM-2015/36, (2015). https://doi.org/10.2172/1185903
22. M. Boyard, J.M. Cherel, C. Pascal et al., The Jules Horowitz Reactor core and cooling system design. In Joint Meeting of the National Organization of Test, Research, and Training Reactors and the International Group on Research Reactors, Sept 12–16, (2005), Gaithersburg, MD.
23. International Atomic Energy Agency. Safety margins of operating reactors: analyses on uncertainties and implications for decision making. (2003). TECDOC-1332. https://www-pub.iaea.org/MTCD/Publications/PDF/te_1332_web.pdf
24. F. Peng, Irradiation ability of research and test reactor. In Compilation of literatures on the thirty-year operation of HFETR (1980–2010). Chengdu, Sichuan Publishing Press: 72–75. (in Chinese)

25. Y. Sudo, M. Kaminaga, A new CHF correlation scheme proposed for vertical rectangular channels heated from both sides in nuclear research reactors. J. Heat Trans. **115**(2), 426–434 (1993). https://doi.org/10.1115/1.2910695
26. Y. Sudo, Study on critical heat flux in rectangular channels heated from one or both sides at pressures ranging from 0.1 to 14 MPa. J. Heat Trans. **118**(3), 680–688 (1996). https://doi.org/10.1115/1.2822686
27. A.E. Bergles, W.M. Rohsenow, The determination of forced-convection surface-boiling heat transfer. J. Heat Trans. **86**(3), 365–372 (1964). https://doi.org/10.1115/1.3688697
28. F.W. Dittus, L.M.K. Boelter, Heat transfer in automobile radiators of the tubular type. Int. Commun. Heat. Mass. **12**(1), 3–22 (1985). https://doi.org/10.1016/0735-1933(85)90003-X
29. J.H. Wang, Analysis of HFETR shut down state caused by loss of off-site power supply. Nucl. Power Eng. **18**(3), 217–220 (1997). (**in Chinese**)
30. W.X. Tian, S.Z. Qiu, G.H. Su et al., Accident analysis of station blackout for China advanced research reactor with shutdown failure. Nucl. Power Eng. **29**(03), 59–63 (2008). (**in Chinese**)